Int. J. Electrochem. Sci., 11 **(2016)** 5063 – 5079, doi: 10.20964/2016.06.8

International Journal of
ELECTROCHEMICAL
SCIENCE
www.electrochemsci.org

Influence of Electrochemical properties on Surface Micromorphology of Zn-Al-Mg-RE alloy coatings

Kai Guo[1,2] , *Xingeng Li*[1,2,*], *Xiaoming Wang*[1,2], *Zengwu Yue*[1,2], *Yishu Du*[3], *Fengjie Yan*[1,2], *Suhong Chen*[1,2], *Jianmei Cao*[1,2], *Wenjing li*[1,2], *Yaping Wu*[1,2]

[1] Materials Laboratory of State grid corporation of china, Jinan, 250002, PR china.
[2] State Grid Shandong Electric Power Research Institute, Jinan, 250002, PR china.
[3] State Grid HeZe power supply company, HeZe, 274000, PR china.
[*]E-mail: lxgeng@126.com

Received: 18 February 2016 / *Accepted:* 5 April 2016 / *Published:* 4 May 2016

Zn-Al-Mg-RE series hot-dip alloy coatings developed which provide effective protection of mild steel surface against corrosion and oxidation were investigated by Scanning Electron Microscopy (SEM), 3D Optical Microscopes, X-ray diffraction (XRD). Significant variation in coating surface morphology, polarization parameters and impedance characteristics are observed with increasing content of Al and Mg element in this paper. It is found that the charge transfer resistance of electrode reaction (R_{ct}) has an inversely proportional relationship with the surface corrosion roughness (R_a) of corroded coatings. Furthermore, the better corrosion resistance derived from certain eutectic reaction in Zn-Al-Mg-RE alloy eutectic process has been indicated in terms of this dynamic relationship. The complex effects on independent processes from initial uncorroded surface microstructure changes in characteristics during and after electrochemical measurement have been represented for different compositions of alloy coatings.

Keywords: Zn-Al-Mg-RE alloy; alloy coatings; electrochemical; microstructure; corrosion rate; surface

1. INTRODUCTION

Zinc-Aluminum series coatings have been widely proved to provide effective sacrificial protection of steel surface against environmental corrosion in virtue of its high corrosion resistance with a comparatively small coating weight [1-4]. Because of the increasing requirements for a long service life in the power steel members and other industries, various alloy systems have been developed. Zn-Al-Mg series coatings have attracted attention since they are shown to be able to

provide corrosion resistance stability superior to that of traditional Zinc and Zn-Al series coatings [5,6]. Many papers are preferential attracted with the periphery of the α-Al phase which is prepared from baths containing more than 6 mass% Al [7,8]. The coating corrosion resistance has been grown along an increase in the content of Mg within the range of 0 mass% -3 mass% though lots of researches [3,9,10]. Several commercial products for heavy corrosive building applications, such as Zn-11Al-3Mg-0.2Si (Super Dyma), Zn-6Al-3Mg (ZAM), have been available through 1990s by Japanese [11,12]. In the last 10 years, Many European research groups have started to develop unique coating systems [13-16]. Some researchers found that the corrosion was inhibited by the buffering of the pH by the formation of layered double hydroxides precipitation of $Al(OH)_3$ in Zn-Al series coatings [17]. They attributed this factor to the enhanced corrosion performance to the stabilizing of the corrosion products in presence of Mg^{2+} ions. Some other points proposed that the prevention of Zinc carbonate hydroxide formation due to cation hydrolysis on the surface [8,13]. Corrosion behaviors of Zn-Al-Mg coatings in chloride and different anions containing environments have already been investigated [11,14,18]. However, the contribution to coating corrosion resistance of the electrochemical properties and the microstructure of morphology is not clear. Different polarization parameters, phase compositions and surface roughness may lead to variation of corrosion resistance. It becomes more and more important to understand the corrosion mechanism of Zn-Al-Mg-RE coatings, because reliable predictions are needed. The aim of this work is to investigate the significant variation in the coating micromorphology, polarization parameters and impedance characteristics with the influence of Al, Mg and RE element. Although, there are already some understanding on the corrosion mechanism of Zn-Al-Mg coatings in the polarization corrosion tests and other studies. To get a novel overview of the corrosion behavior in terms of the charge transfer resistance of electrode reaction (R_{ct}) test and surface corrosion roughness (R_a) would be helpful to give an indication of corrosion performance in a real application. More importantly, a dynamic linear relationship between the charge transfer resistance of electrode reaction (R_{ct}) and surface corrosion roughness (R_a) has been established, which indicates better corrosion resistance derived from the certain eutectic reaction microstructure in Zn-Al-Mg-RE alloy solidification process.

2. EXPERIMENTAL DETAILS

Mild steel panel specimens of dimensions 50 mm×50 mm×5 mm，100 mm×50 mm×5mm, having composition Si-0.16, C-0.18, Mn-0.65, P-0.026, Mo-0.015, Ni-0.02 (all in mass%) and the rest of iron, were used as the substrate materials. The specimens were degreased with 10% NaOH aqueous solution at 50℃ for 2min, and then the oxide scale of samples surface was removed with 20% HCl aqueous solution for 1.5min. A 52%$ZnCl_2$+$SnCl_2$+NaF (9:1:3) solution was developed to immerse the mild steel panel at 80℃ for 20 s, and then they were putted in drying box at 100℃. After drying, the specimens were hot-dipped in Zn (99.99% purity) bath, Zn-5Al bath, Zn-Al-Mg-RE alloy bath, respectively, at 460 ℃～480 ℃for 50 s～120 s. The composition of coatings which were formed in different alloy series and its characteristic parameter are given in Table 1.

Table 1. The composition and characteristic parameter of different zinc-based coatings used in the study.

Materials	Zn	Zn-Al	Zn-Al-RE	Zn-Al-Mg	Zn-Al-Mg-RE		
					Z-5A-1M	Z-5A-2M	Z-6A-3M
Al (mass %)	0～0.2	5±0.5	5±0.5	6±0.5	5±0.5	5±0.5	6±0.5
Mg (mass %)	-	-	-	3±0.2	1±0.1	2±0.2	3±0.2
RE (mass %)	-	-	0.1±0.05	-	0.1±0.05	0.1±0.05	0.1±0.05
Thickness (μm)	95±5	85±5	80±5	70±5	75±5	75±5	70±5

The coatings are all produced in self-made hot dipping equipment. After hot-dipping in alloy baths, the specimens were cooled in air and then quenched in cool water for 50 s～100 s.

The Surface morphology and cross-sectional microstructure of Zn-Al-Mg-RE coatings were examined by using Scanning Electron Microscope (SEM). The phases in the hot-dip coatings were analyzed by XRD using Oxford diffractometer with Cu Kα (λ= 1.54060Å) incident radiation. The peaks of XRD were recorded in the 2θ range of 10º-100º.

Dynamic Polarization and electrochemical impedance experiments were performed using PARSTAT 2273 Advanced Electrochemical System (USA)at the open circuit potential. Polarization measurements were carried out from a cathodic potential of -250 $mV_{(SCE)}$ to an anodic potential +250 $mV_{(SCE)}$ at room temperature (25℃) with respect to corrosion potential. The experiments were conducted in the 3.5 mass% NaCl at a sweep rate 1 mV/s. PowerSuite software was used for data acquisition and analysis. The electrodes were prepared by leaving areas for exposure to the electrolyte about 1 cm^2. The corrosion potential (E_{corr}) and corrosion current density (I_{corr}) and polarization corrosion rate (V_{corr}) were determined by using Tafel extrapolation method. The charge transfer resistance of electrode reaction (R_{ct}) was obtained from Nyquist polt by fitting the data using PowerSuite software.

In particular, surface morphology characteristics of different coatings after electrochemical corrosion measurements were established by using 3D Optical Microscopes (Bruker, GT-K), using VSI mode, with 5 mm×5 mm area. The surface corrosion roughness (R_a) of coatings was carried out in morphology analysis.

3. RESULTS AND DISCUSSION

3.1. XRD analysis of coatings surface

Fig. 1 shows the measured XRD pattern obtained of the coatings with different contents of Al, Mg, RE. The measurement results in Fig. 1 (a) represents Zn, (b) for Zn-5%Al, (c) for Zn-5%Al-

0.1%RE, (d) for Zn-5%Al-1%Mg-0.1%RE, (e) for Zn-5%Al-2%Mg-0.1%RE, (f) for Zn-6%Al-3%Mg, (g) for Zn-6%Al-3%Mg-0.1%RE, respectively.

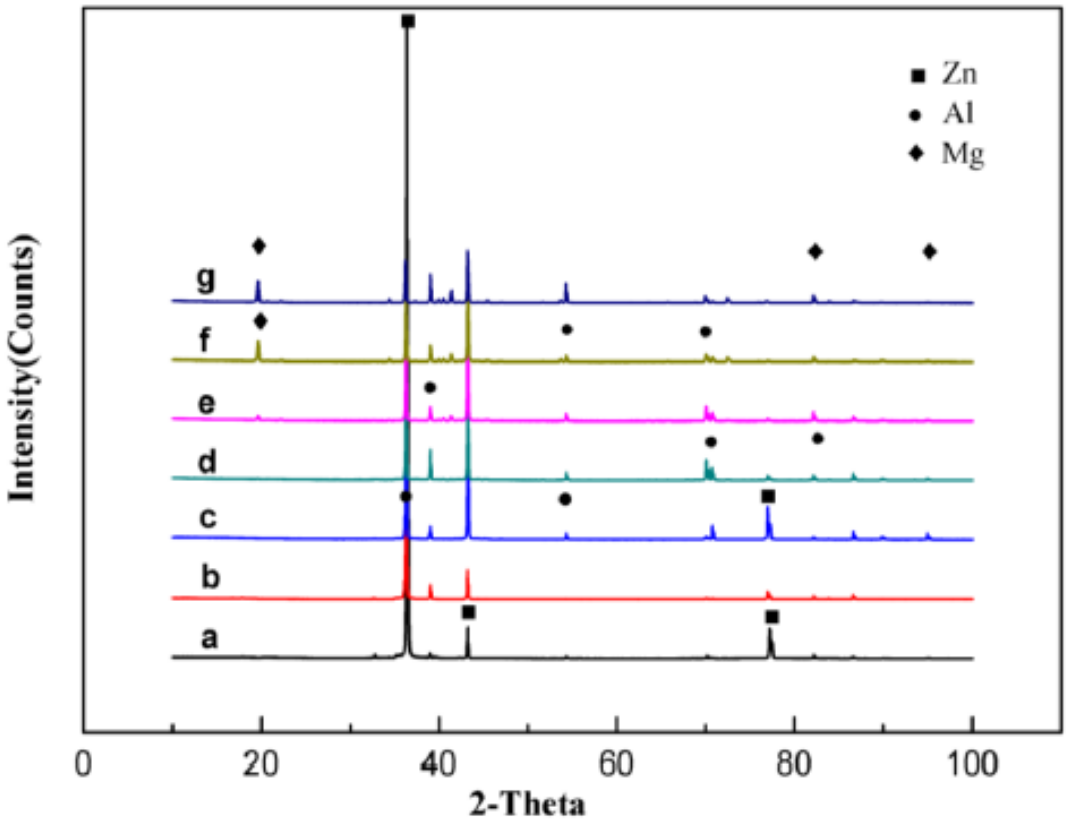

Figure 1. XRD patterns of Zn-Al-Mg-RE coatings, (a) Zn, (b) Zn-5%Al, (c) Zn-5%Al-0.1%RE, (d) Zn-5%Al-1%Mg-0.1%RE, (e) Zn-5%Al-2%Mg-0.1%RE, (f) Zn-6%Al-3%Mg, (g) Zn-6%Al-3%Mg-0.1%RE.

The reduction in the columnar Fe-Zn compound content is attributed to the inhibiting effect of Al when compared to pure zinc coating [2,19]. Zn-Al phase consists of the lamellar eutectic of zinc containing approximately 5% aluminium [22]. As seen from the result, it is probable that Zn-Al-Mg coatings are composed of primary Zn dendrites, Zn-$MgZn_2$ binary eutectic and Zn-Al-$MgZn_2$ ternary eutectic [20,21]. The intensity of the peak due to Zn-6%Al-3%Mg, Zn-6%Al-3%Mg-RE consists of a large amount of primaryα-Al phase, $MgZn_2$ crystals and ternary Zn-Al-$MgZn_2$ eutectic.

3.2. SEM of coatings surface micromorphology

The surface morphology images of the coatings were shown in Fig. 2. The well-crystallized coatings are observed from the pure zinc baths at 450℃ for 1min as shown in Fig. 2(a). With increasing the content of Al to 5 mass%, the Zn-Al bath shows a significant effect on the reduction in the size of zinc crystals. This effect increase the number of eutectic group, or primary Zinc-rich phase

and hypoeutectic structure, or primary α-Al phase and the hypereutectic structure composed of primary α-Al phase and eutectic [23], as shown in Fig. 2 (b). It is evident that the incorporation of Al in Zn-Al bath increases the degree of crystalline coverage through reducing the grain size of the zinc coating compared with-out it. The rare earth element in the Zn-Al-RE baths show a significant effect on the addition in the distribution of the eutectic group, or primary Zinc-rich phase, or primary Al-rich phase crystals. This feature enables the rapid activation at the surface of mild steel substrate and increases the number of micro eutectic sites which speeds up the eutectic evolution reaction as seen in Fig. 2(c).

The increase in magnesium causes the conversion of ternary eutectic reaction to improve the corrosion resistance with the subsequent outer alloy layer matrix of the Zn-Al-Mg coatings. Instead of a few crystals growing small, many eutectic groups grow to a larger size on average. There are also some dark areas are presented in the layer matrix which are rich in Al and Mg. Those areas are surrounded by a brighter phase which contains similar amounts of Zn or Fe. The microstructure of the coatings surface formed in the bath with Zn-5%Al-2%Mg-RE is more uniform and the crystal clusters arranged together more compactly than that formed in Zn-5%Al-1%Mg-RE baths as presented in Fig. 2(d) and (e). However it is not observed that the large ternary eutectic of Zn-Al-$MgZn_2$ is formed and the morphology of coatings is not uniform, while the cracks are also observed. The possible reason is that the scanty amount of magnesium would restrain the ternary eutectic reaction.

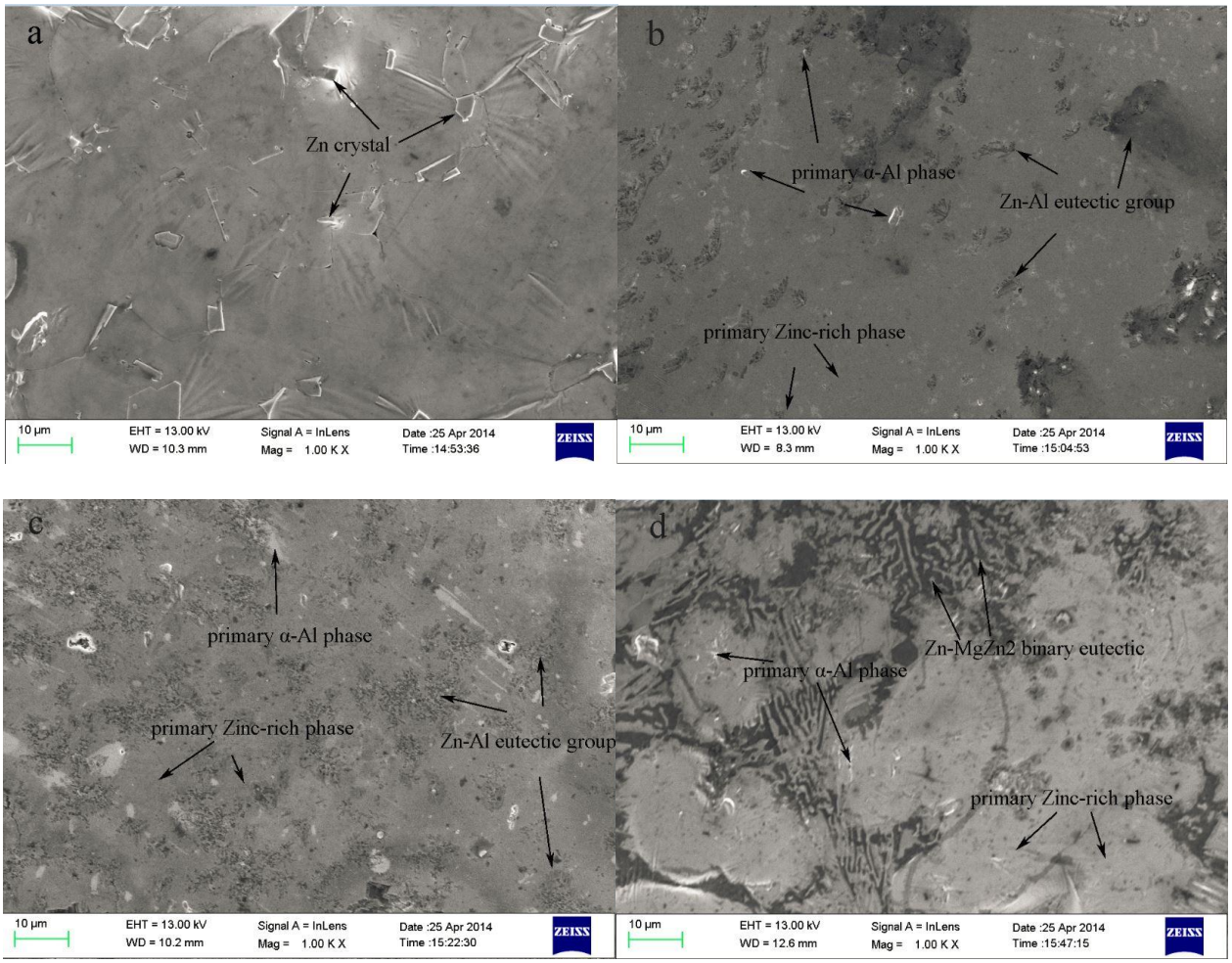

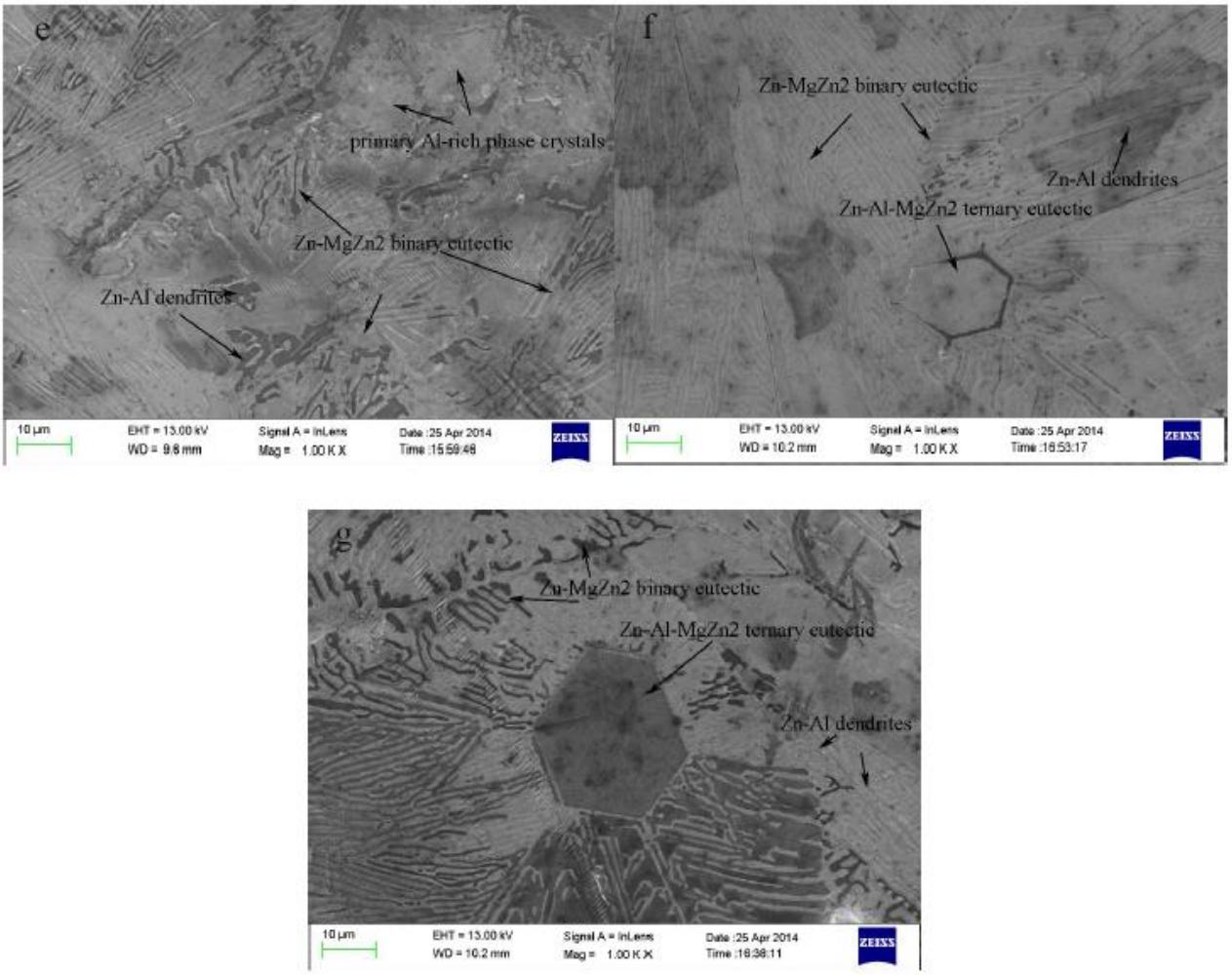

Figure 2. SEM images of Zn-Al-Mg-RE coatings surface, (a) Zn, (b) Zn-5%Al, (c) Zn-5%Al-0.1%RE, (d) Zn-5%Al-1%Mg-0.1%RE, (e) Zn-5%Al-2%Mg-0.1%RE, (f) Zn-6%Al-3%Mg, (g) Zn-6%Al-3%Mg-0.1%RE.

The crystal clusters of coatings obtained from the baths containing Mg with 3 mass% are denser and larger than others. In Fig. 2(f) and (g), some dark areas are primarily α-Al and some bright areas are eutectic structure of Zn-Al and α-Al. By comparison, the optimum amount of Mg increases the number of nucleation sites there by increasing the number of ternary eutectic group. The rare earth element in the Zn-Al-Mg-RE bath shows a significant effect on the addition in distribution of the ternary eutectic group. It is found that the size of ternary eutectic Zn-Al-$MgZn_2$ and Al dendrites in the Zn-6%Al-3%Mg-RE coatings as presented in Fig. 2(f) are better organized than that of the Zn-6%Al-3%Mg coating in Fig. 2(g). The Zn-6%Al-3%Mg-RE coating has a multiphase structure with Zn-$MgZn_2$ binary eutectic and Zn-Al dendrites. There are also zones of ternary eutectic Zn-Al-$MgZn_2$ and Al dendrites [24,25]. In general, the larger the size of the crystals, the higher coverage and more effective coatings are obtained by Zn-6%Al-3%Mg-RE bath.

3.3. Electrochemical properties

3.3.1. Dynamic polarizationPotentiodynamic Polarization

A typical potentiodynamic polarization technique is used to evaluate the protectiveness of the coatings in 3.5% NaCl solution at room temperature. From the anodic polarization curves as shown in Fig. 3, corrosion potential (E_{corr}), corrosion current density (I_{corr}) and the corrosion rate (V_{corr}) derived from these curves are given in Table 2.

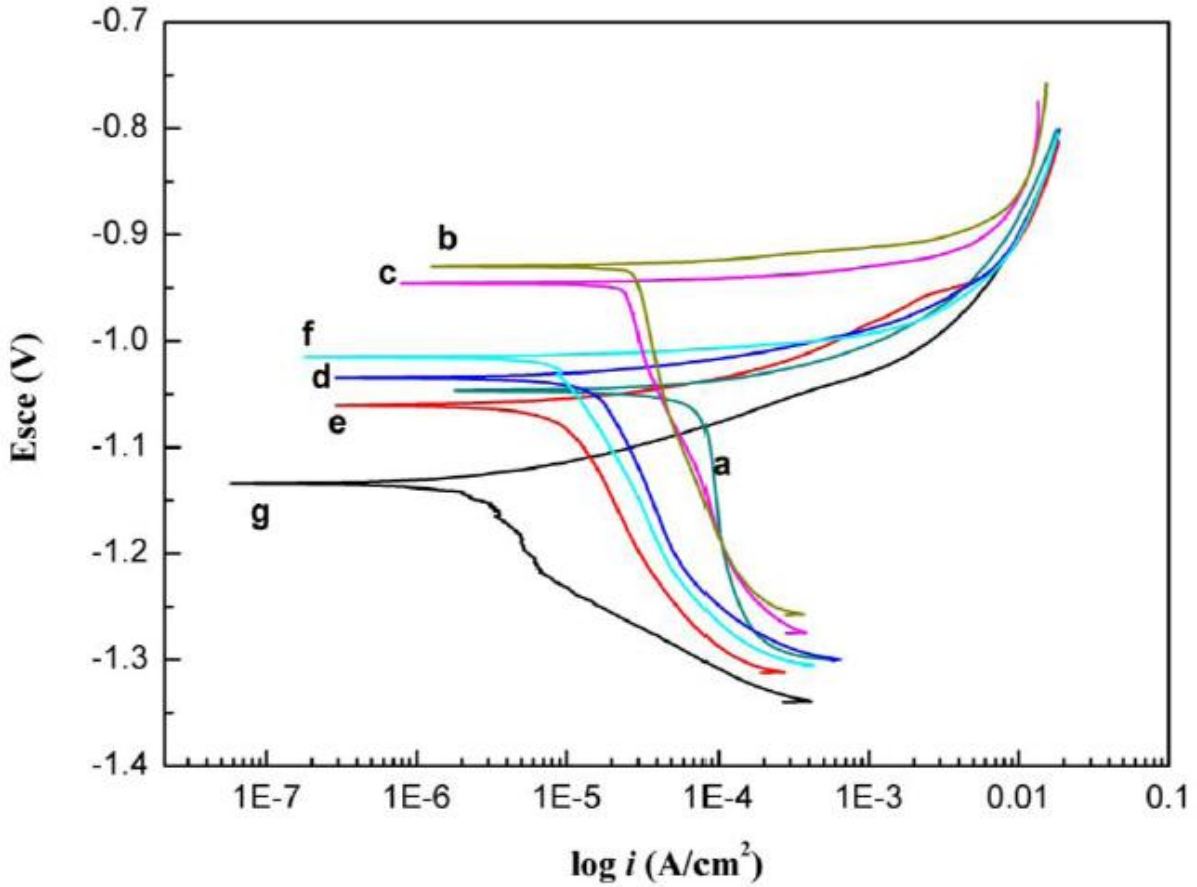

Figure 3. Tafel polarization curves of mild steel samples deposited with Zn-Al-Mg-RE coatings, (a) Zn, (b) Zn-5%Al, (c) Zn-5%Al-0.1%RE, (d) Zn-5%Al-1%Mg-0.1%RE, (e) Zn-5%Al-2%Mg-0.1%RE, (f) Zn-6%Al-3%Mg, (g) Zn-6%Al-3%Mg-0.1%RE.

It is evident from Fig. 3 that the corrosion potential has been shifted towards less negative values for the Zn-Al coatings developed in the presence of Al. Among the relevant studies, the substrate with Zn-Al coatings prepared from hot-dip baths has shown the lower corrosion current density and the lower corrosion rate which means the more positive corrosion resistance [26]. Those could be attributed to the formation of eutectic group or the hypereutectic structure composed of primary Al-rich phase and the reduction in the columnar Fe-Zn compound content. As shown in Fig. 3, the extent of shift in E_{corr} is largely a function of the rough-and-tumble in alloy coatings.

The polarization curves of coatings which are developed in the presence of magnesium ranging from 0 mass% to 3 mass% show some marked difference compared to coatings developed in the absence of Mg. A larger shift of E_{corr} and I_{corr} in the positive direction is observed when the concentration of Mg increases from 2 mass% to 3 mass%. The transform come from electrochemical corrosion to the substrateis hindered by the protection of ternary alloy layer between the substrate and the electrolyte. Those coatings are generally denser and finer than others, which will decreases the average polarization corrosion rate considerably. The decrease in the corrosion current for Zn-Al-Mg series clearly indicate that the coating is more uniform and less cracks than the zinc and Zn-Al coatings. The polarization curve emphasizes the effect of Mg on the corrosion resistance of Zn-Al-Mg coatings developed on mild steel substrate. The optimum concentration (3 mass%) in the alloy bath leads to the denser morphology which results in the formation of the multiphase structure with Zn-$MgZn_2$ binary eutectic and Zn-Al dendrites, or ternary eutectic Zn-Al-$MgZn_2$ and dendrites crystals [27]. The significant changes of polarization parameters are arriving at the polarization zone per unit area in meantime depending on the small amount of rare earth element.

With help of potentiodynamic polarization, corrosion rates (V_{corr}) are measured as seen in Table 2.

Table 2. Corrosion rate (V_{corr}) and I_{corr}, E_{corr} for mild steel samples coated with different content obtained in the 3.5 mass% NaCl at room temperature.

Sample mass%	E_{corr} (V VS SCE)	I_{corr} (A/cm^2)	Anode Tafel slopes (V/decade)	Cathodic Tafel slopes (V/decade)
(a)pure Znic	-1.079	1.415×10^{-4}	0.038	-0.405
(b)Zn-5%Al	-0.935	1.006×10^{-4}	0.011	-0.658
(c)Zn-5%Al-0.1%RE	-0.947	6.72×10^{-5}	0.008	-0.251
(d)Zn-5%Al-1%Mg-0.1%RE	-1.035	4.36×10^{-5}	0.019	-0.313
(e)Zn-5%Al-2%Mg-0.1%RE	-1.072	0.786×10^{-5}	0.019	-0.281
(f)Zn-6%Al-3%Mg	-1.013	0.413×10^{-5}	0.008	-0.227
(g)Zn-6%Al-3%Mg-0.1%RE	-1.228	0.275×10^{-5}	0.039	-0.176

Due to the eutectic and dendrites group on the surface of Zn-Al-Mg coatings, it displays a better corrosion resistance than the coatings without Mg. Those indicate that these coatings prevent as much as possible reactions at its interface in alloy baths. More importantly, according to the different anodic/cathodic Tafel slopes of coatings, the Zn-6%Al-3%Mg-RE exhibits the effective corrosion resistances. Comparing with the different coatings, the Zn-6%Al-3%Mg-RE itself own the lost I_{corr} and V_{corr} due to the formation of effective multiphase structure.

3.3.2. Electrochemical impedance characteristics

Comparison of Nyquist plots of Zn, Zn-Al alloy and Zn-Al-Mg-RE coatings in 3.5% NaCl have been shown in Fig. 4.

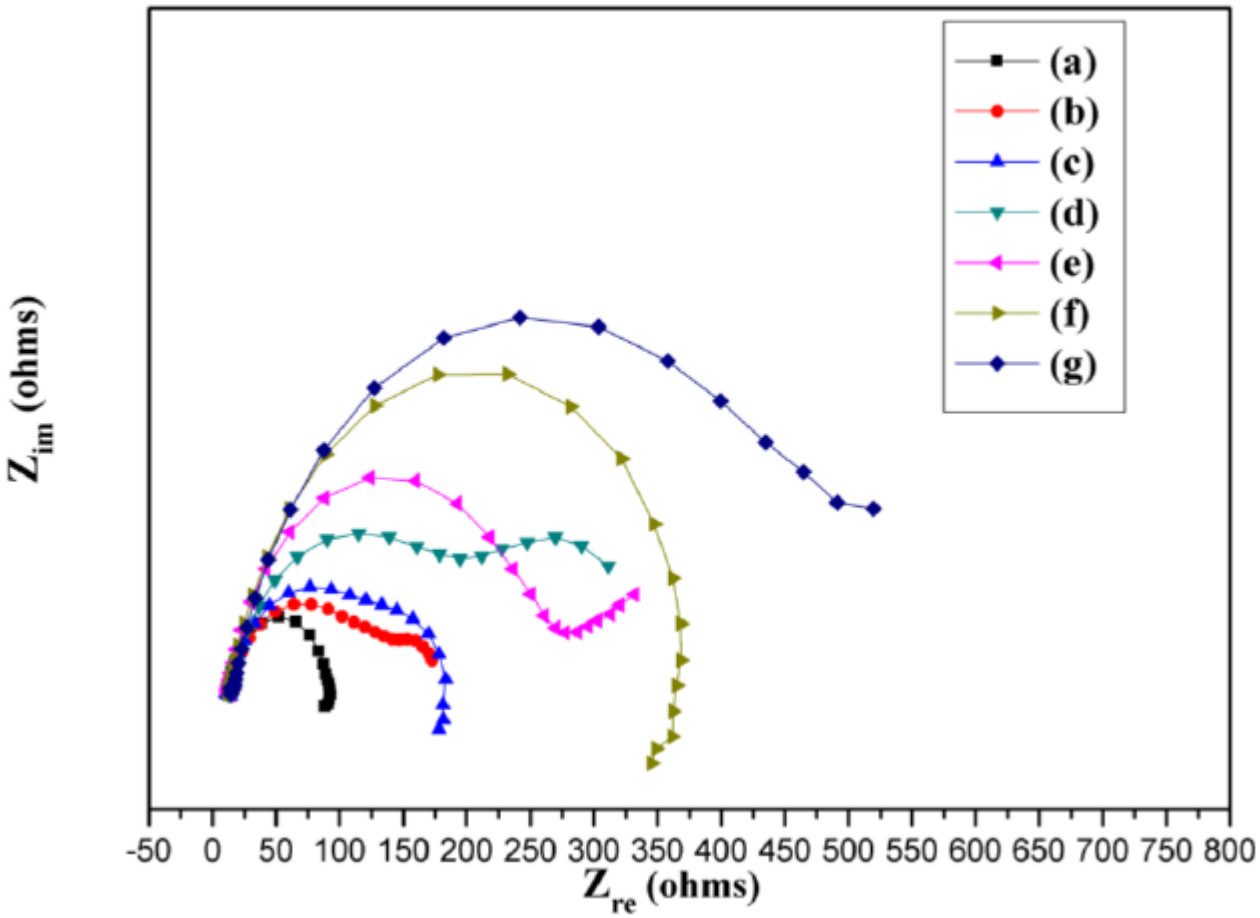

Figure 4. Electrochemical impedance curves of mild steel samples deposited with Zn-Al-Mg-RE coatings, (a) Zn, (b) Zn-5%Al, (c) Zn-5%Al-0.1%RE, (d) Zn-5%Al-1%Mg-0.1%RE, (e) Zn-5%Al-2%Mg-0.1%RE, (f) Zn-6%Al-3%Mg, (g) Zn-6%Al-3%Mg-0.1%RE.

It is clearly found that the size of the curves is increased with increasing magnesium content in the alloy bath from 0 to 3 mass%. This indicates the significant increase in the polarization resistance of those alloy coatings in 3.5% NaCl as presented in Fig. 4(a)-(g), which means that the corrosion resistance of samples with Zn-Al-Mg-RE coatings is improved [28,29]. With the reduction of aluminum, the diameter of the semicircles decreased which means the decrease in the barrier protection.

According to Eq.(1) and the artificial circuit (2) and (3), the charge transfer resistances of electrode reaction (R_{ct}) has been obtained from Nyquist polt by fitting the data using PowerSuite software are given in Table 3. Furthermore, the artificial circuit (2) was used for the Nyquist polt of (a) Zn, (c) Zn-5%Al-0.1%RE, (f) Zn-6%Al-3%Mg and (g) Zn-6%Al-3%Mg-0.1%RE and the artificial circuit (3) was used for others.

$$R_{ct} = \frac{RT}{nFi_0} \quad (1)$$

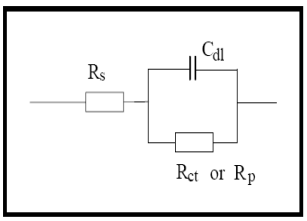

(2)

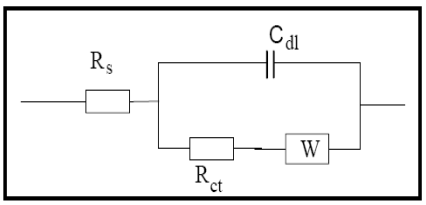

(3)

The charge transfer resistances of electrode reaction (R_{ct}) which As Al content increasing to 5 mass% in Zn-Al bath results in the reduction of micro cracks which lead to the addition of eutectic group at the coatings surface, and those phenomenon lead to improve the corrosion resistance. However, they have some disagreements with the results of polarization measurements.

Table 3. The charge transfer resistance of electrode reaction (R_{ct}) for samples coated with different content obtained in the 3.5 mass% NaCl at room temperature.

Sample mass%	R_c ($\Omega \cdot cm^2$)	C_{dl} ($F \cdot cm^2$)	Charge transfer resistance (R_{ct}) ($\Omega \cdot cm^2$)
(a) pure Znic	4.852	11.76	156.8
(b)Zn-5%Al	4.686	14.42	208.4
(c)Zn-5%Al-0.1%RE	4.912	8.97	237.1
(d)Zn-5%Al-1%Mg-0.1%RE	4.384	18.72	270.8
(e)Zn-5%Al-2%Mg-0.1%RE	4.496	16.94	264.2
(f)Zn-6%Al-3%Mg	4.108	19.85	295.6
(g)Zn-6%Al-3%Mg-0.1%RE	3.985	21.32	297.3

Because of the corrosion product and the reactant will be transported during the electrochemical corrosion reaction, the reaction resistance is improved with increasing magnesium content as seen in Fig. 4. The protective effect of alloy coatings will be greater when optimum concentration of magnesium is included in the Zn-Al-Mg bath by supporting the formation of the more multiphase structure in coatings. According to the different Nyquist plots of coatings, Zn-6%Al-

3%Mg-RE exhibited the largest charge transfer resistance of electrode reaction (R_{ct}) due to the formation of effective multiphase structure. The multiphase structure with Zn-$MgZn_2$ binary eutectic and ternary eutectic Zn-Al-$MgZn_2$ will be formed during the addition magnesium to 3 mass%, thereby it displays a better corrosion resistance than the other coatings. As we know, the corrosion potential (E_{corr}), corrosion current density (I_{corr}), corrosion rates (V_{corr}) and charge transfer resistance of electrode reaction (R_{ct}) are widely used to characterize the electrochemical properties of Zn-Al-Mg-RE coatings. However, the E_{corr} is chaotic and does not have the well-organized relation with the changes of Al and Mg. Furthermore, all those parameters are fussy and complicated to express the different electrochemical corrosion properties with different content Zn-Al-Mg series coatings. More importantly, we aim to obtain a kinetic relationship between electrochemical parameters and the changes of coatings surface in corrosion process.

3.4. Coatings micromorphology after electrochemical corrosion

The coatings micromorphology images of Zn-Al, Zn-Al-Mg series coatings after electrochemical corrosion were shown in Fig.5. It is observed that the dissolution of coatings surface has happened. Zn coating surface has been widely corroded which has been shown in Fig. 5(a). Comparing with Zn-Al series coatings, Zn coating tend to be corroded much faster and heavier. The increasing degree of crystalline coverage and reducing of the size of the zinc crystals will promote the corrosion resistance properties of coatings layer, which can been found in the surface changes after corrosion as shown in Fig. 6(b). With the addition of rare earth element in Zn-Al bath, the number of etch pit have been significant reduced by comparing the surface states difference of Zn-5%Al and Zn-5%Al-RE in Fig. 6(b) and (c). However, there are some deep etch pits in the surface of Zn-5%Al series coatings, which may lead to the further corrosion. Those characteristics could result in the poor corrosion resistance of Zn-5%Al series coatings. Due to the conversion of ternary eutectic reaction by adding magnesium, the corrosion resistance has been remarkable improved and remained uncorroded after electrochemical corrosion. Fig. 6(d) and (e) show the changes in micromorphology of the outer layer with corrosion for both Zn-5%Al-1%Mg-RE and Zn-5%Al-2%Mg-RE coatings.

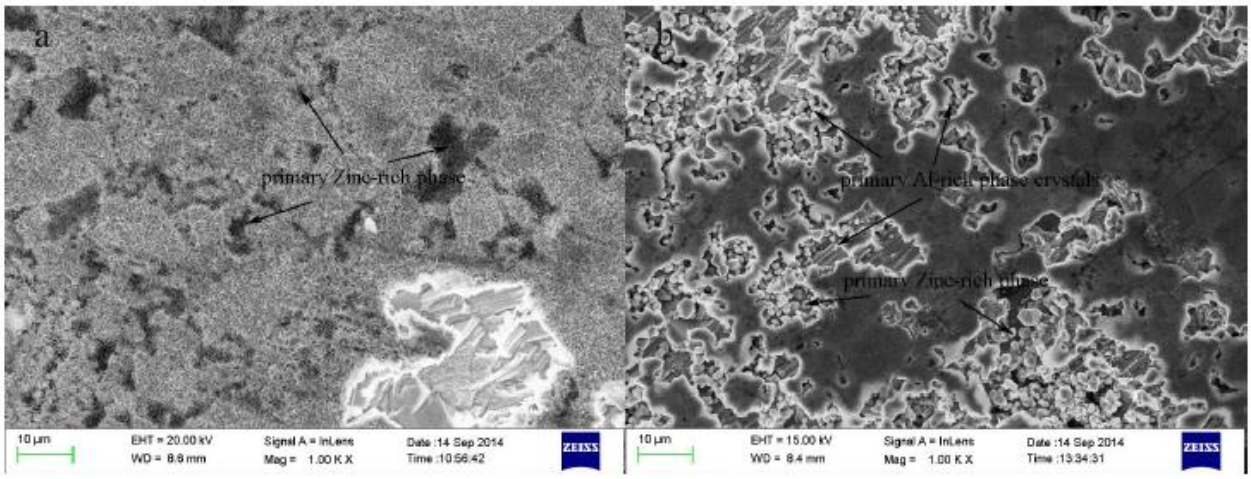

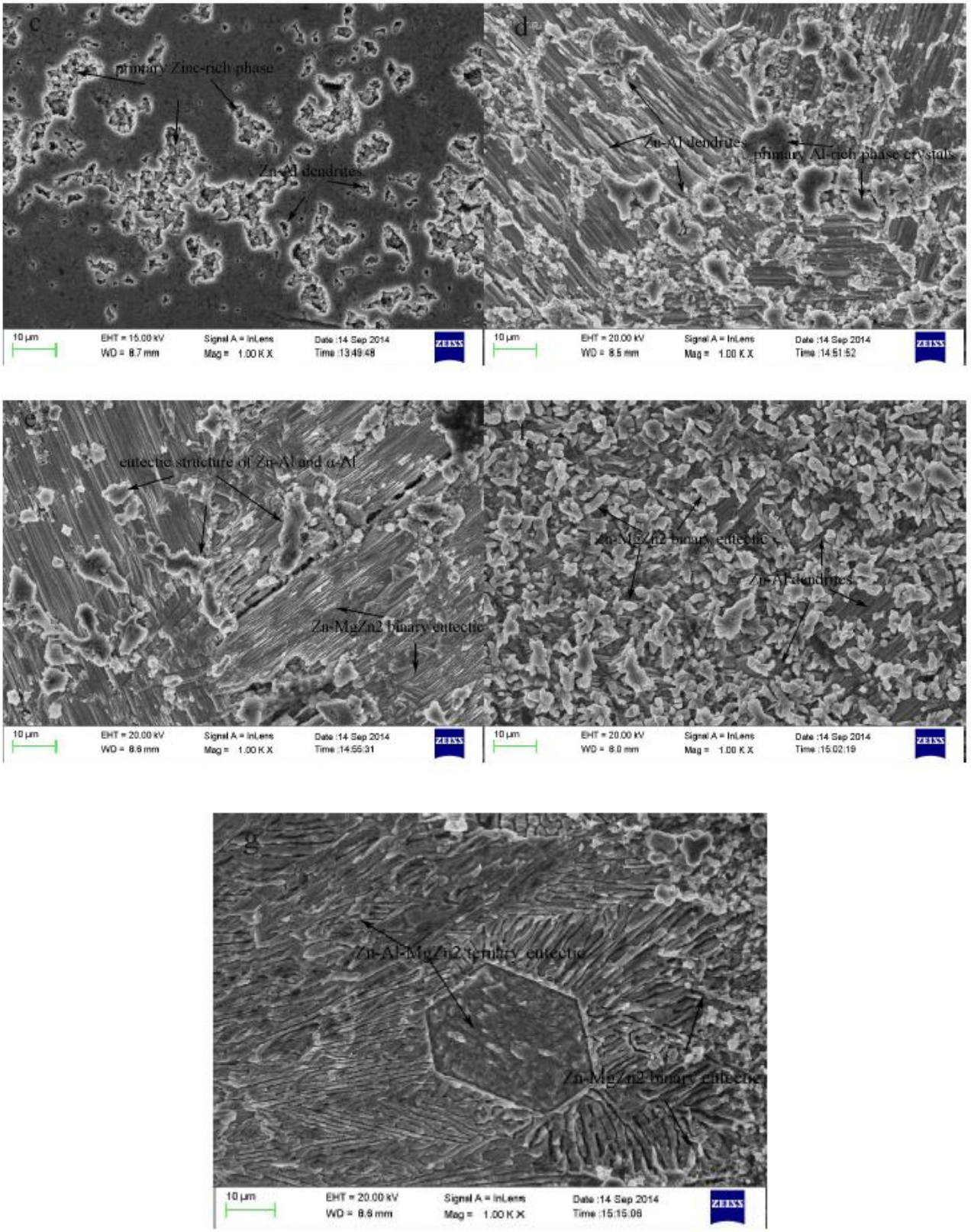

Figure 5. SEM images of Zn-Al-Mg-RE coatings surface after Electrochemical corrosion, (a) Zn, (b) Zn-5%Al, (c) Zn-5%Al-0.1%RE, (d) Zn-5%Al-1%Mg-0.1%RE, (e) Zn-5%Al-2%Mg-0.1%RE, (f) Zn-6%Al-3%Mg, (g) Zn-6%Al-3%Mg-0.1%RE.

As shown above, the denser and larger crystal clusters of coatings with 3 mass% Mg in Fig. 6(f) and (g) lead to the corrosion resistance improvement. The larger size of ternary eutectic Zn-Al-$MgZn_2$, Al dendrites and more uniform ternary eutectic microstructure have been preserved by comparing with Zn-6%Al-3%Mg and Zn-6%Al-3%Mg-RE. Those lead to the Zn-6%Al-3%Mg-RE exhibit effective electrochemical corrosion resistant.

3.5. Three-Dim Optical microstructure

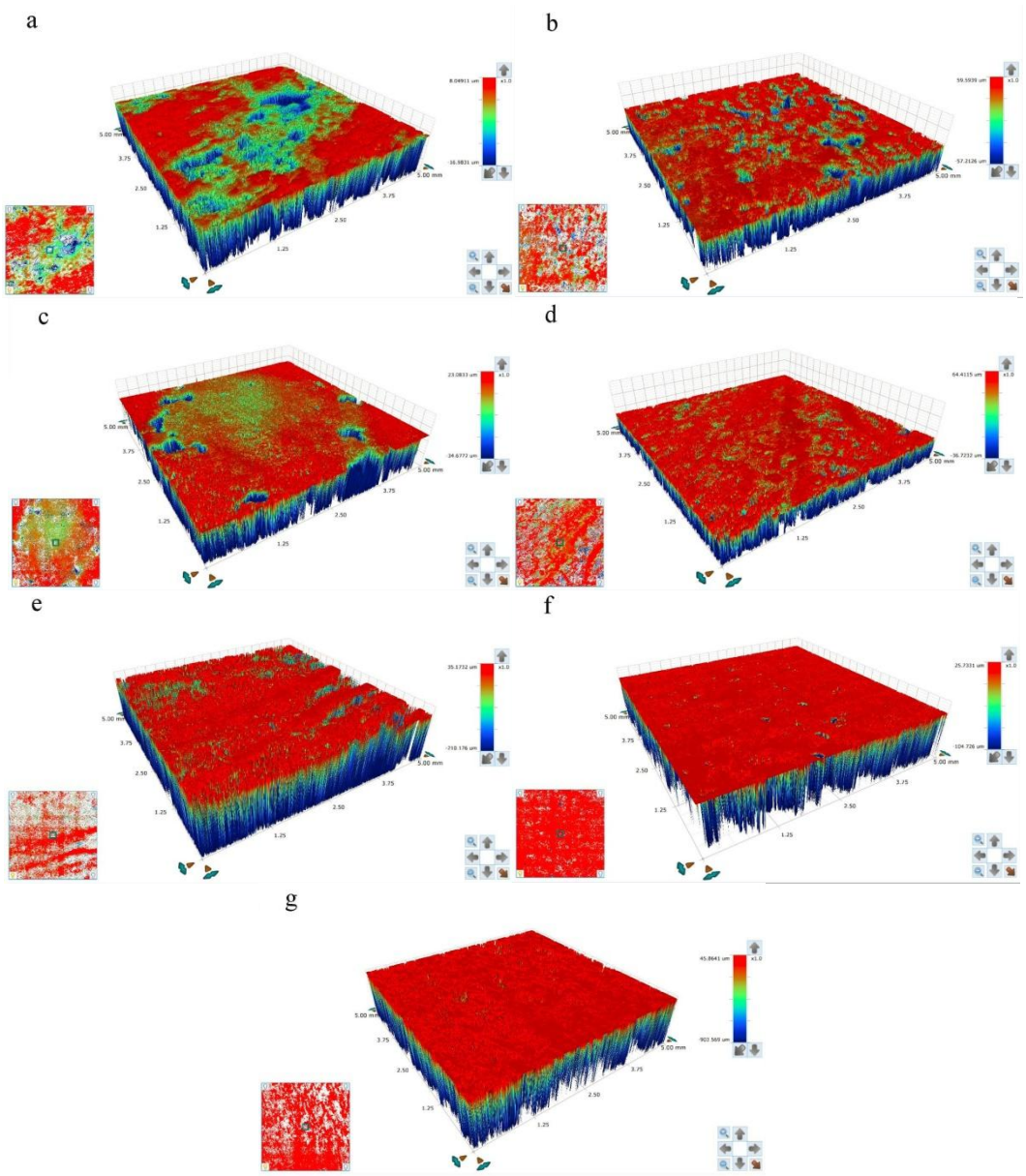

Figure 6. 3D Optical Microscopes images of Zn-Al-Mg-RE coatings surface after electrochemical corrosion measurement, (a) Zn, (b) Zn-5%Al, (c) Zn-5%Al-0.1%RE, (d) Zn-5%Al-1%Mg-0.1%RE, (e) Zn-5%Al-2%Mg-0.1%RE, (f) Zn-6%Al-3%Mg, (g) Zn-6%Al-3%Mg-0.1%RE.

Fig.6 shows the surface microstructures changes in characteristics for different compositions of the coatings using the 3-D optical profilometry after electrochemical corrosion measurement. All figures are organized to illustrate the changes between independent samples covering an area of 5mm by 5mm. The colour zones displayed in the figures indicate distance from the lowest point within the pits, as shown by shades of blue, to the highest point, as shown by the reds.

It is observed that the dissolution of coatings surface layer has been taken place during anodic polarization and cathodic polarization. At the same time, the porosity has been increased, which will ultimately result into corrosion of the electrolyte. The dark parts are the preferentially corroded areas of Zn coating in Fig. 6(a). It is clearly seen that this coating tend to corrode much faster and heavier than the Zn-Al coatings shown in Fig. 6(b) and (c). With increasing the content of Al to 5 mass%, corrosion has been initiated at the bound areas between zinc crystal clusters and eutectic group, or primary Zinc-rich phase and hypoeutectic structure, or primary Al-richphase and the hypereutectic structure [30]. The increasing degree of crystalline coverage and reducing of the size of the zinc crystals promote the corrosion resistance properties of coatings layer, which can been found in the changes of surface corrosion roughness (R_a) as shown in Table 4. A significant effect which is caused by addition of rare earth element in the Zn-Al-RE bath has been observed comparing with the surface states difference of Zn-5%Al and Zn-5%Al-RE in Fig. 6(b) and (c). According to the conversion of ternary eutectic reaction to improve the corrosion resistance by adding magnesium, corrosion takes place only in α-Al crystals and their periphery. However, the ternary eutectic structure remained uncorroded. Fig. 6(d) and (e) show the changes in microstructures of the outer layer with corrosion for both Zn-5%Al-1%Mg-RE and Zn-5%Al-2%Mg-RE coatings. The decrease in pits represents the improved corrosion resistance due to the conversion of ternary eutectic reaction through increasing magnesium content.

The crystal clusters of coatings obtained from the Zn-Al-3 mass% Mg alloy baths are denser and larger than others according to the SEM microstructure. Those surface structures have effective corrosion resistance capability as presented in Fig. 6(f) and (g). With the larger the size of the multivariate eutectic structures, the Zn-6%Al-3%Mg-RE itself own the lowest surface corrosion roughness (R_a) and exhibit the most outstanding surface morphology. As the further corrosion proceeding, the strong Zn-$MgZn_2$ binary eutectic, Zn-Al dendrites and zones of ternary eutectic Zn-Al-$MgZn_2$, Al dendrites maintain the almost original structure. Accordingly, the incorporation of 3 mass% Mg and 0.1 mass% rare earth element in to the Zn-Al-Mg-RE bath has remained crystal unchanged and also helped to achieve effective surface corrosion resistance ability. However, the relationship between electrochemical parameters and surface corrosion roughness (R_a) of coatings surface after electrochemical measurement has not been established in previous study which may reflect the changes in the different stages of corrosion.

3.6. Kinetic relationship

Through the classical electrochemical measurement and surface morphology analysis, the corrosion properties of Zn-Al-Mg-RE coatings have been well explored. Based on the different I_{corr},

V_{corr}, R_{ct}, and R_a during the electrochemical corrosion process, the inverse linear relationship between R_{ct} and R_a has been established to reveal the corrosion connection of the initial uncorroded coatings and microstructures changes in characteristics for different coatings during electrochemical corrosion process. The higher R_{ct} represents the better electrochemical corrosion resistant properties and the complex effects on the corrosion resistant ability due to the formation of multiphase structure with Zn-$MgZn_2$ binary eutectic, Zn-Al dendrites and ternary eutectic Zn-Al-$MgZn_2$ and Al dendrites as mentioned above**.** More importantly, R_{ct} shows the inverse relationship with surface corrosion roughness (R_a) of coatings as increasing Al and Mg content. The relationship between R_a and R_{ct} for different compositions of the coatings is shown in Fig. 7. With the lower $R_{a,}$ the corrosion resistance ability of alloy coatings surface will be better. However, with higher R_{ct}, electrochemical corrosion resistant properties of different compositions of alloy coatings will be relevantly enhanced.

Generally, the different contents of alloy coatings have direct connection with their surface microstructure and electrochemical properties. However, the complex cross-linked relationship via the corrosion reaction and the cumbersome polarization, impedance analysis in electrochemical corrosion process do not help us to understand the dynamic connection between initial electrochemical corrosion parameters and finally corroded coatings surface characteristics. It is considered that the negative linear relationship between R_{ct} and R_a represents the crosslinking effects on the independent different corrosion process from the initial uncorroded surface to the corroded microstructure during the electrochemical measurement.

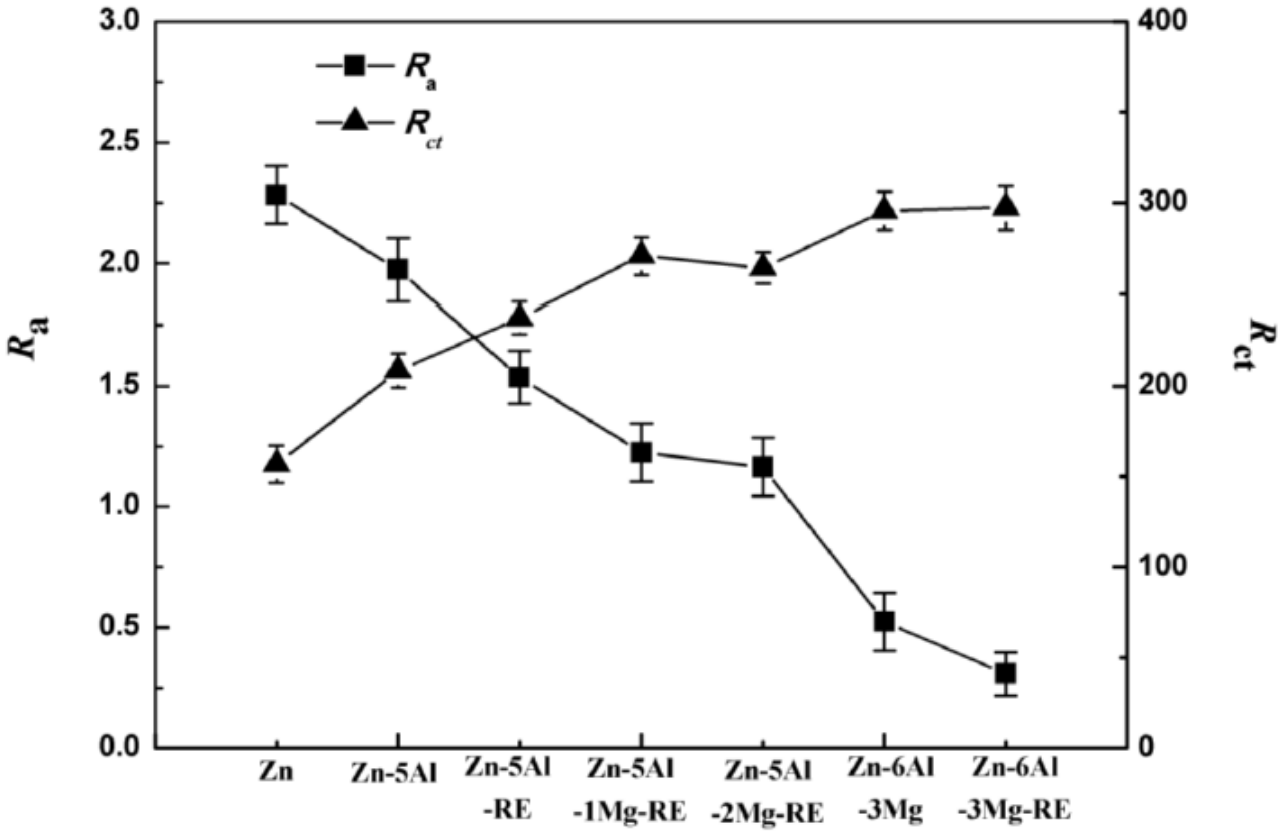

Figure 7. Relationships between R_{ct}, R_a and the different compositions of Zn-Al-Mg-RE series coatings.

4. CONCLUSION

In this work, the significant variation in the coatings micromorphology changes, polarization parameters and impedance characteristics are observed with the different compositions of Zn-Al-Mg-RE series coatings. According to our experiment results, the inverse linear relationship has been established in terms of the charge transfer resistance of electrode reaction (R_{ct}) and the surface corrosion roughness (R_a). The lower R_a and the higher R_{ct} indicates the better corrosion resistance derived from the certain eutectic reaction microstructure in the Zn-Al-Mg-RE solidification process. This relationship represents the complex influences of independent electrochemical corrosion processes to the microstructure change characteristics for different compositions of Zn-Al-Mg-RE coatings during electrochemical measurement. Furthermore, this inversely-proportional relationship might be applied to other alloy coatings to understand their kinetic relationships between surface corrosion and electrochemical properties.

ACKNOWLEDGEMENTS
This work was supported by the scientific research project of State Grid Corporation of China.

References

1. P. Puomi, H.M. Fagerholm, J.B. Rosenholm, *Anti-Corrosion Method Material*, 46 (1999) 163-172.
2. M.Vlot, R. Bleeker, T. Malman, E.vanPerlstein, *Galvanized Steel Sheet Forum, Dusseldorf* (2006).
3. R. P. Edavan, R. Kopinski, *Corrosion Science*, 51 (2009) 2429-2442.
4. R. Hausbrand, M. Stratmann, M. Rohwerder, *Steel Research International*, 74 (2003) 453-458.
5. J. Sullivan, D. Penneya, J. Elvinsb, K. Khana, *Surface & Coating technology*, 16 (2016) 25-36.
6. Li Qian, Zhao Yang-zi, LuoQun, *Jounal of alloy and compounds*, 501 (2010) 282-290.
7. F. Crea, C. De Stefano, D. Milea, S. Sammartano, *Journal of Solution Chemistry*, 38 (2009) 115.
8. T.Prosek a, D.Persson, J.Stoulil, D. Thierry, *Corrosion Science*, 86 (2014) 231-238.
9. M. Dutta, A. K. Halder, S. B. Singh, *Surface & Coating technology*, 205 (2010) 2758-2584.
10. N. LeBozec, D. Thierry, A. Peltola, L. Luxem, G. Luckeneder, G. Marchiaro, M.Rohwerder, *Material Corrosion*, 64 (2013) 969-978.
11. T. Prosek, N. Larche´, M. Vlot, *Material Corrosion*, 61 (2010) 412-420.
12. K. Tano, S. Higuchi. Nip. *Steel Research Report*, 25 (1985) 29-34.
13. T. Prosek, D. Thierry, C. Taxen, J. Maixner, *Corrosion Science*, 49 (2007) 2676-2682.
14. J. Hirmke, M. X. Zhang, D. H. StJohn, *Surface & Coating technology*, 206 (2011) 425-433.
15. J. Duchoslav, M. Arndt, R. Steinberger, T. Keppert, G. Luckeneder, K.H. Stellnberger, *Corrosion Science*, 83 (2014) 327-334.
16. N. LeBozec, D. Thierry, M. Rohwerder, D. Persson, G. Luckeneder, L. Luxem, *Corrosion Science*, 74 (2013) 379-386.
17. P. Volovitch, T.N. Vu, C. Alley, *Corrosion Science*, 53 (2011) 2437-2346.
18. R.M. Cigala, F. Crea, C. De Stefano, G. Lando, D. Milea, S. Sammartano, *Journal of Chemical and Engineering Data*, 55 (2010) 4757.
19. V. Ezhilselvi, J. Nithin, J. N. Balaraju, S. Subramanian, *Surface & Coating technology*, 288 (2016) 221-229.
20. E. de Bruycker, Z. Zermout, B.C. De Cooman, *Material Corrosion*, 539 (2007) 1276-1281.
21. R. Hausbrand, M. Stratmann, M. Rohrwerder, *Jounrnal of Electrochemistry. Society*, 155 (2008) C369-C379.

22. J. Duchoslava, M. Arndta, R. Steinbergera, T. Keppertb, G. Luckenederb, K.H. Stellnbergerb, *Corrosion Science*, 83 (2014) 327-334.
23. S. Sugimaru, S. Tanka, Nip. *Steel technology Report*, 96 (2007) 34-38.
24. W. Yuansheng, X. Ji, *Surface & Coating technology*, 206 (2011) 1277-1282.
25. C. Zhong, W.B. Hu, Y.M. Jiang, B. Deng, J. Li, *Journal of Coatings Technology and Research*, 8 (2011) 107.
26. A. Jimenez, J. Negrete, G. Villasenor, *Material Characteristic*, 61 (2010) 1286-1289
27. S. Ranganatha,T.V. Venkatesha, K. Vathsalab, M. K. Punith kumara, *Surface & Coating technology*, 208 (2012) 64-72.
28. M. Tamilselvi, P. Kamaraj, M. Arthanareeswari, *Applied Surface Science*, 332 (2015) 12-21.
29. M. Dutta, A. K.Halde, S. B. Singh, *Surface & Coating technology*, 205 (2010) 2578-2584.
30. J. Klein, J. Schneider, M.Muske, *Thin Solid Film*, 451 (2004) 481-484.